

Development and application of future design weather data for evaluating the building thermal-energy performance in subtropical Hong Kong

Sheng Liu^{a,*}, Yu Ting Kwok^a, Kevin Ka-Lun Lau^{b,c,d}, Hong Wai Tong^e, Pak Wai Chan^e, Edward NG^{a,b,c}

^a School of Architecture, The Chinese University of Hong Kong, AIT Building, New Territories, Hong Kong

^b Institute of Future Cities, The Chinese University of Hong Kong, New Territories, Hong Kong

^c Institute of Environment, Energy and Sustainability, The Chinese University of Hong Kong, New Territories, Hong Kong

^d CUHK Jockey Club Institute of Ageing, The Chinese University of Hong Kong, New Territories, Hong Kong

^e Hong Kong Observatory, Kowloon, Hong Kong

ARTICLE INFO

Article history:

Received 15 July 2019

Revised 20 November 2019

Accepted 10 December 2019

Available online 17 December 2019

Keywords:

Climate change

Morphing method

Building energy simulation

Adaptive thermal comfort

Future weather data

ABSTRACT

To better understand the impacts of the warming caused by global climate change on building performance, future hourly weather data that account for climate change are crucial to building simulation studies. Downscaling from general circulation models (GCMs) by the morphing method has been adopted by researchers worldwide. Using this method, we developed six sets of future hourly weather data for Hong Kong, taking the typical meteorological year (TMY) as the baseline climate. The ensemble mean from 24 general circulation models (GCMs) in the Coupled Model Intercomparison Project Phase 5 (CMIP5) has also been incorporated to take into account the uncertainties and biases between different models. These newly developed future weather data were then employed in the building energy simulation to evaluate the impacts of future climate change. Moreover, this study used the adaptive comfort standard (ACS) from ASHRAE Standard 55 in a mixed-mode residential building to consider the acclimatization effects of occupants in the changing climate. Results indicate that by the end of this century, the indoor discomfort percentage in the cooling seasons are expected to increase from 21.9% for TMY to 36.0% and 50.4% under RCP4.5 and RCP8.5 scenarios, respectively, while the annual cooling load is expected to increase up to 278.80%.

© 2019 Elsevier B.V. All rights reserved.

1. Introduction

Climate change is a widely acknowledged environmental issue affecting society, ecosystem and our built environment. The Intergovernmental Panel on Climate Change (IPCC) concluded that up to about 30% and 40% of the worldwide greenhouse gas (GHG) emissions and energy consumption come from the building sector [1]. IPCC also pointed out that the energy saving potential and reduction of GHG emissions in the building sector is one of the most cost-effective approaches to mitigate climate change. It should be noted that the worsening climate may cause the increase of building energy consumption and subsequently GHG emissions that can further exacerbate the global warming. Therefore, actions from the

building sector to mitigate and adapt to climate change are crucial to reduce the building energy consumption and GHG emissions.

To facilitate the impact analysis, the IPCC developed future climate scenarios (A1, A2, B1 and B2), contained in the Special Report on Emissions Scenarios (SRES), to investigate the uncertainty of future GHG emissions and the diversity of driving forces [2]. The SRES scenarios were used in the 2007 IPCC Fourth Assessment Report (AR4) [3]. At the end of 2014, IPCC published the Fifth Assessment Report (AR5), in which it recommends the adoption of the new generation of scenarios based on the integration of socio-economic and climate scenarios in future climate change research and impact assessments [1]. The projection making in AR5 used the Representative Concentration Pathways (RCP). Four scenarios were selected to represent different pathways of GHG emissions and atmospheric concentrations, namely, RCP2.6, RCP4.5, RCP6.0, and RCP8.5 [4]. Compared to the SRES, the RCPs are largely underpinned by the assumption that different portfolio of activities and measures could result in the radiative forcing characteristics

* Corresponding author.

E-mail address: sheng.liu@link.cuhk.edu.hk (S. Liu).

Nomenclature

ACS	Adaptive Comfort Standard
AR	Assessment Report
ASHRAE	American Society of Heating, Refrigerating, and Air-Conditioning Engineers
CanESM2	Canadian Earth System Model
CMIP	Coupled Model Intercomparison Project Phase
GCMs	General Circulation Models
GHG	Greenhouse Gas
HadCM3	Hadley Center Coupled Model Version 3
HKO	Hong Kong Observatory
HVAC	Heating, Ventilation and Air Conditioning
IAQ	Indoor Air Quality
IPCC	Intergovernmental Panel on Climate Change
OTTV	Overall Thermal Transfer Value
PMV	Predicted Mean Vote
PRH	Public Rental Housing
RCMs	Regional Climate Models
RCP	Representative Concentration Pathways
SRES	Special Report on Emissions Scenarios
TMY	Typical Meteorological Year
TRY	Typical Reference Year
WCRP	World Climate Research Programme
T_{ao}	Outdoor Air Temperature of Each Calendar Month
$T_{o,up80}$	Upper 80% Acceptability Limits of Indoor Operative Temperature

by 2100 [5]. There is not an appreciable divergence of the radiative forcing in different RCPs until after the near-term (2035). However, even in the most optimistic and stringent mitigation scenario (RCP2.6), the global mean surface temperature by the end of this century is still likely 1.7 °C higher than the period 1985–2005 [1].

The building envelope essentially works as a mitigation shelter to moderate the outdoor natural environment for creating optimum conditions of livability. When buildings are confronting the worsening weather conditions caused by climate change, overheating of the indoor environment may result due to the higher ambient temperature, solar heat inputs, and convective and conductive heat gains through the building envelope [6]. In buildings without proper passive design strategies, the rising temperature and climatic anomalies may contribute to the excessive thermal discomfort and even cause heat-related health problems for the occupants [7]. Under those circumstances, the more frequent usage of mechanical cooling is inevitable, further increasing the energy consumption in buildings [8]. With reference to a large number of studies on the correlation between the ambient temperature and the cooling demand, Santamouris [9] calculated that the increase of cooling load in typical urban buildings for the period 1970–2010 is close to 23% at the global scale. By estimating the increase of the residential and commercial building floor areas in 2050 based on the average development scenarios of world population, it was calculated that the average cooling energy demand will significantly increase up to 750% and 275% for the residential and commercial buildings, respectively [10]. At the regional scale, the highest residential cooling energy demand is expected in Asian countries after 2050 because of the penetration of air conditioning in the future, the population increase, and global climate change. For instance, the residential energy demands in China and India are predicted to reach 1610 TWh and 4700 TWh in 2100, respectively [11]. In particular, in the hot summer and warm winter climates, where building energy consumption is dominated by space cooling, the most significant impacts of climate change on the building energy demand would occur in this climate classification compared to the

other regions [12]. Thus, the significant increase of residential cooling energy consumption in these areas is expected to make the building sector be the dominant energy component in the future.

1.1. Methods for evaluating the building energy impacts of climate change

Many previous studies have evaluated the impacts of climate change on building energy use. Quantitative analyses on the impacts of climate change on building energy use have gained attention since the end of the last century [13,14]. The methodology commonly used in the earlier studies is the degree-day-based technique that assumes an appropriate regression relationship between the cooling/heating degree hours and the annual energy use in buildings [15]. This technique is widely used to analyze the weather-induced changes in building energy use. However, the degree-day-based method does not include the other meteorological variables, e.g., solar radiation, humidity, nor the building characteristics. Consequently, there are often large deviations in predicted building energy use when compared to numerical simulations [8]. More importantly, the adaptation strategies and technologies considered for the building design are rather limited in this method.

With the help of dynamic simulation tools, e.g., EnergyPlus, DOE-2 and ESP-r, the building energy consumption can be simulated based on more detailed hourly weather data, including the dry- and wet-bulb temperatures, wind speed, solar radiation, and etc. In the past, the typical reference year (TRY) or typical meteorological year (TMY) data are employed in building energy simulations to represent the typical weather conditions recorded. Hence, the change of climatic conditions is not contained in the historical data. In 2005, Belcher et al. [16] first developed a statistical downscaling method, known as the morphing method, to construct the hourly weather data for future climates by statistical downscaling from atmosphere-ocean general circulation models (GCMs). With the hourly weather data incorporating climate change effects, researchers are able to evaluate the specific impacts of climate change on building energy consumption [17]. Thanks to the morphing method, the impacts of increasing temperature on the building energy consumption and indoor overheating risks have been studied globally in the last decade. For instance, in the United States, Wang and Chen [8] projected the rate of change in energy demand for various building types through EnergyPlus simulations using the future hourly weather data by morphing projections from the Hadley Center Coupled Model Version 3 (HadCM3). Similarly, Shen et al. [18,19] adopted two scenarios, namely, A2 and A1F1 in the AR4, from the HadCM3 GCM based on the morphing method to investigate the impacts of climate change on building energy consumption in four different climate zones in the United States. In Brazil, Triana et al. [20] evaluated the thermal and energy performance of social houses using the future weather file generated from the CCWorld-WeatherGen tool, which was developed by Jentsch et al. [17] from the University of Southampton in 2013 based on the HadCM3 model from the AR4. With the help of the same CCWorld-WeatherGen tool, Pagliano et al. [21] used validated building energy model of a child care center in Milan (Italy) to investigate the changes in building energy use and uncomfortable thermal conditions. The results showed that the space cooling and duration of discomfort in summer will be the major challenges in the future. In Iran, Roshan et al. [22] examined the effects of future climate on the different cooling and heating strategies by downscaling the Canadian Earth System Model (CanESM2) GCM, and revealed that the use of cooling strategies in the future will increase. In Taiwan, Huang and Hwang [23] first produced future hourly weather data for building energy simulations by using the morphing method and adopted the adaptive comfort model to con-

sider the operation mode of air-conditioning in a mixed-mode residential building. They revealed that the cooling energy of typical residential buildings in Taiwan will increase by 82% in 2080s under the A1B scenario. Hwang et al. [24] then explored the impacts of climate change on the building envelope energy conservation index of typical office buildings in Taiwan by adopting RCP4.5 scenarios from CanESM2.

As the IPCC suggested that no single model can represent the best projection due to the varied biases of different GCMs, it is necessary to use the results from multiple model rather than a single model to consider the uncertainties of models [25]. In the morphing method, the projected monthly-mean change from the GCMs should be integrated into the existing TMY hourly weather data as the input for building energy simulations. Although this method has been commonly used worldwide, most of the aforementioned studies only used a small number of models and scenarios or a single model with multiple scenarios.

1.2. Climate change and building energy consumption in Hong Kong

Hong Kong (22°19'N, 114°10'E) is located in the subtropical region and experiences a long summer with hot and humid conditions, and the Köppen-Geiger classification subtype of Hong Kong is "Cfa" (Humid Subtropical Climate) [26]. In recent years, under the synergy effects of global climate change and local urbanization, there is a worsening trend of weather conditions in Hong Kong. Recent temperature records showed a continuously increasing trend with a rate of 0.17 °C per decade between 1989 and 2018. In 2018, the annual mean temperature reached 23.9 °C, which is 0.6 °C higher than the mean record from 1981–2010. A new record for May with 15 consecutive very hot days (i.e., days with $T_{\max} \geq 33$ °C) and the annual maximum temperature of 35.4 °C were also observed [27]. All the climate anomalies in the recent years indicated that Hong Kong is not immune to climate change. According to the Hong Kong Energy Saving Plan 2025+ [28], 92.7% of the city's electricity are consumed in buildings and air-conditioning is the largest end-use, accounting for 30% of electricity. This energy demand trend may be attributed to the increasing air-conditioning penetration rate for public (87.06%) and private residential (92.78%) buildings [29], and the high ownership level of 1.67 and 2.66 units per household respectively [30]. As outdoor temperatures continue to rise in the future, the building energy consumption would soar unavoidably. Therefore, mitigation for the impacts of future climate change on the building energy use is a crucial aspect for Hong Kong to meet the 2025 and 2030 energy saving and carbon emission reduction targets [31].

Hong Kong has over 42,000 buildings in its existing building stock, a majority of them are over 30 years old [32], making it particularly sensitive in terms of energy consumption penalty when facing the challenges of climate change. Upon review of the relevant studies in Hong Kong, the major method used for the investigation of how historical or future climate change may impact the energy performance of existing buildings was statistical correlation. For instance, Wong et al. [29] calculated the future cooling load in residential buildings by using a simple correlation between the overall thermal transfer value (OTTV) and the predicted monthly weather data from MIROC3.2-H in the Coupled Model Intercomparison Project Phase 3 (CMIP3). This study also recognized the importance of adaptive thermal comfort for mitigating the rising temperatures in residential buildings. Similarly, using the monthly data from the same MIROC3.2-H, Lam et al. [33] evaluated the effects of future climate change on the increase of energy use in office buildings using regression models with principal component analysis. By using a statistical regression based on the monthly consumption data from 1990 to 2004, Fung et al. [34] estimated that for a 1 °C temperature rise in Hong Kong would cost

HK\$1.6 billion per year on the electricity consumption and the increase rate of the residential sector would be larger than other sectors. The vulnerability of residential buildings in Hong Kong was further confirmed by another study. Ang et al. [35] estimated by regression analysis that the temperature rise in Hong Kong could have the largest effects on energy consumption of the residential sector. Using the data of the residential sector in Hong Kong from 2000 to 2015, another recent study by Morakinyo et al. [36] revealed that the electricity consumption for space cooling per capita and cooling degree day is 0.38 kWh/°C.

To cope with the more frequent climatic anomalies in the future, the vulnerability of residential buildings in Hong Kong would inevitably lead to higher energy demands. This is the reason why residential buildings were chosen as the subject of research in this study. Due to the scarcity of local future hourly weather files, the numerical simulations of building energy in the above studies lack a physical basis [29,33–36]. In 2011, the first set of future design weather files for Hong Kong was developed by Chan [37] using the downscaled data from a CMIP3 model, MIROC3.2-MED (Japan), by the morphing method. His study indicated that the increase of space cooling in residential flats (24%) will be almost double than that in office buildings (14.3%) by the end of this century.

1.3. Purpose of this study

Until now, the state-of-the-art climate models and RCP scenarios from the Coupled Model Intercomparison Project Phase 5 (CMIP5) database have not been used in the building energy simulation studies in Hong Kong. Since the stringent mitigation scenarios in the IPCC AR5 and the previous SRES of AR4 are not equivalent, and most of the climate change studies in Hong Kong predate the AR5, it is time to update the future design weather data for building thermal-energy simulation using the new scenarios and the corresponding CMIP5 models. Furthermore, instead of using a single model or a small number of models and scenarios, multiple model scenarios should be used to ensure the rigor and sophistication of model scenarios selection [15]. Therefore, it is imperative to consider the probability distributions of the future temperature changes and the uncertainties of model spread by using a multi-model ensemble of numerous GCMs [38]. In this study, we employ the projections driven from 24 models to consider the uncertainties between GCMs under different future climate scenarios.

Most of the previous studies [29,37] used a constant air change rate between indoor and outdoor and a fixed setpoint temperature for air-conditioning, while the commonly used hybrid ventilation mode, also known as mixed-mode, of residential buildings in Hong Kong has been often ignored. A mixed-mode building takes advantage of natural ventilation when the indoor thermal conditions are acceptable and operates air-conditioning when they are not. If the mixed-mode operation and the acclimatization effects of occupant behavior are not considered in simulation studies for residential buildings, the impacts of the outdoor changing climate could be misunderstood. Thus, to more comprehensively understand the effects of the future worsening climate conditions on the performance of residential buildings, this study adopts the adaptive thermal comfort model in the building energy simulation to consider the occupant behavior in mixed-mode residential buildings. This enables architects and policy makers to rethink the impacts of climate change and design more resilient buildings and formulate appropriate building regulations in the context of future climate change.

Set against the above background, this study aims to

1. Develop the future hourly weather data for building thermal-energy simulation using the downscaled data from multiple GCMs in the CMIP5; and

- Evaluate the impacts of climate change on the building energy demand and indoor thermal comfort of mixed-mode residential buildings in Hong Kong using the adaptive thermal comfort model as the thermal comfort criterion.

2. Methodology

2.1. Morphing method and baseline climate

The morphing method is by far one of the most viable and efficient approaches to construct the future hourly weather data for building performance simulations by integrating downscaled data from GCMs [17]. This method has been widely used by researchers to encapsulate the monthly future weather data from GCMs into the existing present-day weather data [16–25]. The morphing process starts with the selection of a set of weather data as the baseline climate which represents the present-day weather sequence. An existing TMY weather data file, developed by the *Finkelstein-Schafer (FS)* statistical method based on the observed weather data by Hong Kong Observatory (HKO) from 1979 to 2003 [39], was selected to represent the baseline climate. Subsequently, the baseline climate was morphed using the projected monthly-mean climatic variables, including monthly horizontal solar irradiance and monthly maximum, minimum, and mean dry bulb temperature and wet bulb temperature, from the CMIP5 GCMs under different scenarios. Three generic algorithms are commonly involved in the morphing technique *shift*, *stretch* and *combination of shift and stretch*:

- (1) A *shift* by Δx_m , the absolute change in the monthly mean value of the climatic variable for the month m , is applied to the present-day climatic variable x_0 of the baseline scenario by

$$x = x_0 + \Delta x_m \quad (1)$$

- (2) A linear stretch of α_m is applied by

$$x = \alpha_m x_0 \quad (2)$$

Where α_m is the fractional change in the monthly-mean climatic value for month m . This approach is commonly used when the change of variables is only quoted as a fractional change rather than an absolute increment [19]. For example, the solar irradiance will still be zero at night.

- (1) A combination of shift and stretch is obtained by

$$x = x_0 + \Delta x_m + \alpha_m (x_0 - \langle x_0 \rangle_m) \quad (3)$$

The combination algorithm is often applied when both the mean and variance are required to be changed. For example, it can be applied to the dry-bulb temperature, where the daily mean, maximum, and minimum temperatures need to be appropriately reflected.

2.2. Climate models and climate change projections

To consider the uncertainty and divergence amongst the different models and emission scenarios, or in other words to separate signal from noise, this study adopts a prudent approach which considers the outputs from multiple CMIP5 models under different scenarios when preparing the data for downscaling [40,41]. The outputs of global climate simulations from 24 CMIP5 models on a monthly basis were obtained from the HKO (see Table A1 in Appendix). The detailed daily and monthly experimental outputs under historical and future climate scenarios were extracted from the World Climate Research Programme's (WCRP) CMIP5 multi-model dataset at the Program for Climate Model Diagnosis and Intercomparison website (<http://pcmdi9.llnl.gov>). The outputs of the RCP emission scenarios from 24 CMIP5 models were selected

to be further validated by the historical weather data using the cross-validation approaches. The whole validation process of GCM datasets has been well documented in the previous papers by Chan and Tong [42,43]. It is verified that the historical observed data of HKO over the period 1961–2005 can be reasonably reproduced by the ensemble mean of 24 models. The results are also comparable with previous literature derived by CMIP5 and regional climate models (RCMs) in Southern China [44,45], as well as the previous projection study using AR4 data [40]. Fig. 1 illustrates the projected decadal temperature anomalies of the different GCMs under different scenarios. The mean, standard deviation (σ), and range of temperature anomaly in each decade under the different RCP scenarios are summarized in Table A2 in Appendix. It reveals that ensemble mean projections of the different RCP scenarios are statistically indistinguishable before mid-century (2040–2049), but will become divergent by the end of this century (2090–2099). The ensemble means are 1.24 °C and 1.18 °C for RCP2.6, 1.36 °C and 2.06 °C for RCP4.5, 1.01 °C and 2.35 °C for RCP6.0, and 1.58 °C and 4.03 °C for RCP8.5 in the middle-term and long-term periods, respectively. Moreover, the magnitude of deviation between different GCMs is amplified with time. For instance, the standard deviations of the temperature anomalies of RCP4.5 and RCP8.5 are 0.56 °C and 0.86 °C at the end of the century (2090–2099).

The multi-model ensemble obtained by averaging all models weighted equally was found superior to any one individual model in terms of mean climate [46]. After including a manageable group of models, the stable hindcasts and forecasts can be obtained by averaging all errors across models [47]. In this study, the ensemble means of 24 CMIP5 models under the different RCP scenarios are employed to cover the large uncertainties and biases of different GCMs. It is noteworthy that all the model groups have provided the RCP4.5 and RCP8.5 scenarios, which belong to the core experiments of CMIP5 [41]. Furthermore, the CO₂ emission trajectory of RCP8.5 has been proven to be the closest match with of current path of global CO₂ emission [48] and RCP4.5 scenario is regarded as the most possible scenario among researchers [49]. To reduce the computational costs of simulation works, only the RCP4.5 and RCP8.5 have been selected as the future climate change scenarios considered in the rest of this study. Moreover, the building model is simulated only once during each 20-year period. The projected years in this century are assumed to be divided into three time slices: 2026–2045 as the 2035s, 2056–2075 as the 2065s, 2080–2099 as the 2090s, to represent the near-term, the middle-term and long-term periods, respectively.

After applying the three algorithms of the morphing method, the future hourly design weather data have been generated based on the present-day TMY weather file. For a clearer presentation of the future climate change over this century in Hong Kong, the hourly dry-bulb temperature and relative humidity under the different climate scenarios are plotted according to the psychrometric chart (Figs. 2 and 3). The different colors represent the annual psychrometric distribution over the different time periods, suggesting that cumulative hours located in the hot and humid area are substantially increased over time, especially in the RCP8.5 scenario. It indicates an evident trend of the worsening hot and humid climate in Hong Kong. In the case of temperature, the number of hours above 32.8 °C from April to October in Hong Kong based on the cooling seasons of BEAM Plus [32], which increases from only 3 for the baseline scenario (TMY) to 246 for RCP4.5–2090s and 886 for RCP8.5–2090s, mainly occurring during mid- to late summer from June to September (Table 1). The temperature threshold of 32.8 °C corresponds to the 95th percentile of maximum temperature observed from 2007 to 2014 in Hong Kong. It is in accordance with the worldwide adopted method for defining heat waves for evaluating the heat-related mortality [36].

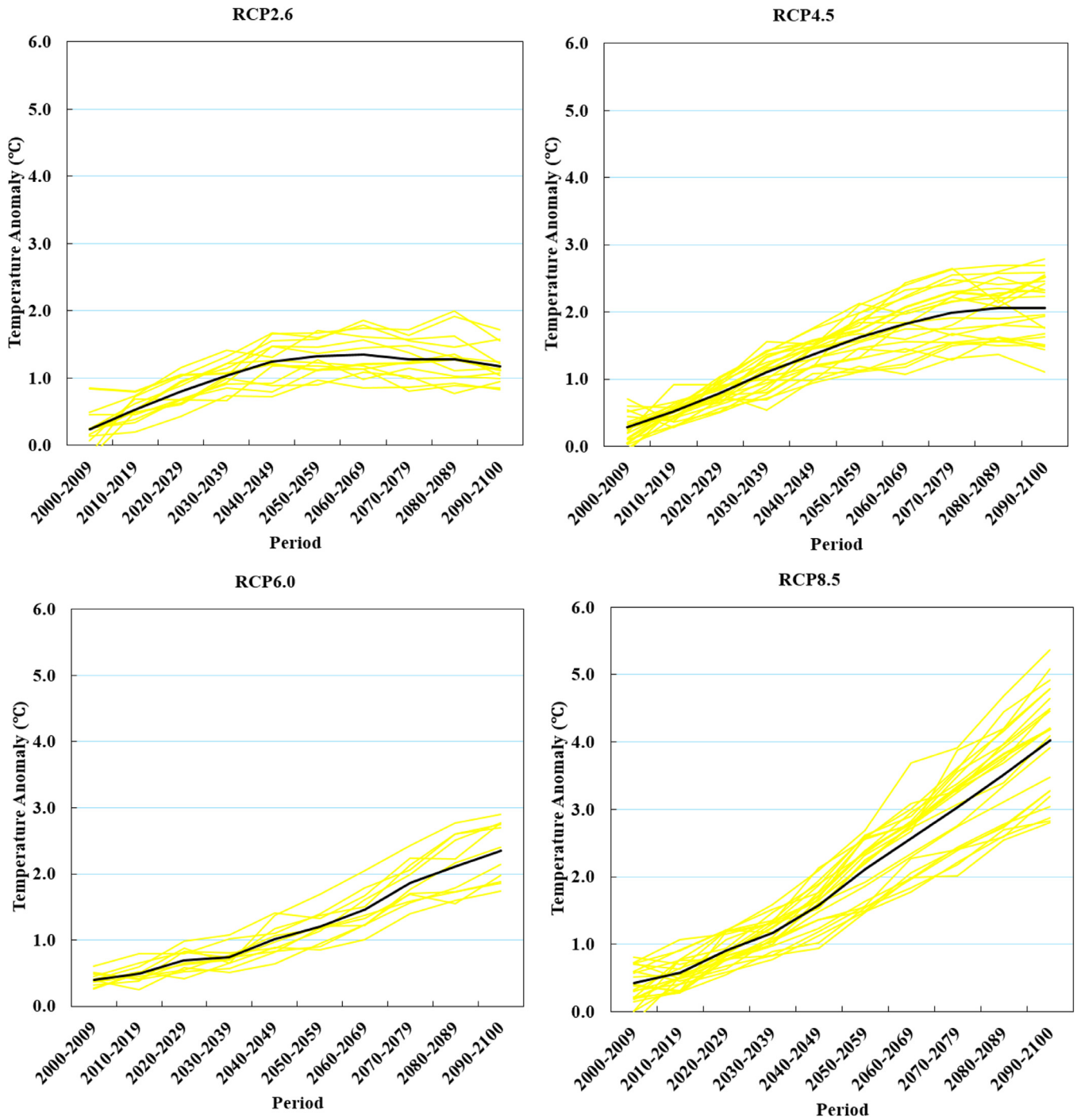


Fig. 1. Projected decadal temperature anomaly of Hong Kong under the different RCP scenarios in the 21st century (relative to the 1979–2003). Each light color curve represents results from a single GCM; the dark curve represents the ensemble mean value from all GCMs considered.

Table 1
Hours beyond the extreme hot temperature ($T_{air} \geq 32.8$ °C).

Period	TMY	RCP4.5			RCP8.5		
	1979–2003	2035s	2065s	2090s	2035s	2065s	2090s
April	0	2	5	6	2	10	30
May	0	0	6	7	0	25	70
June	0	74	93	89	80	122	194
July	1	25	54	46	25	85	165
August	0	35	53	53	38	86	181
September	2	46	41	41	24	79	217
October	0	0	4	4	2	16	29
Total	3	182	256	246	171	423	886

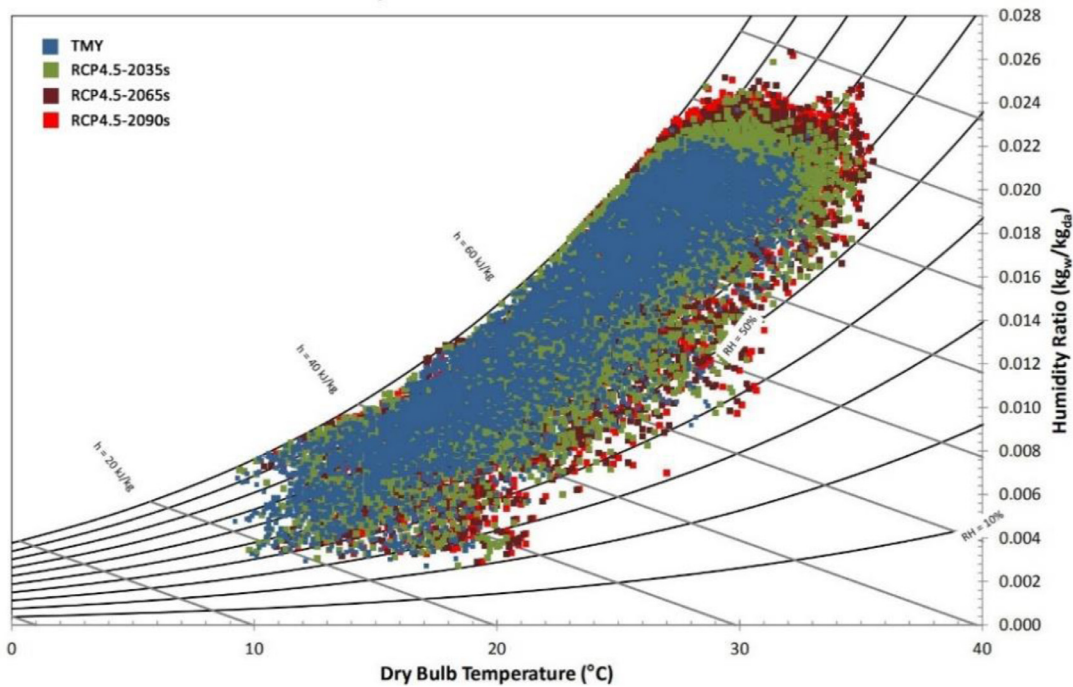


Fig. 2. Psychrometric chart of hourly weather data in the 2035s, 2065s, 2090s under the RCP4.5 and TMY scenarios.

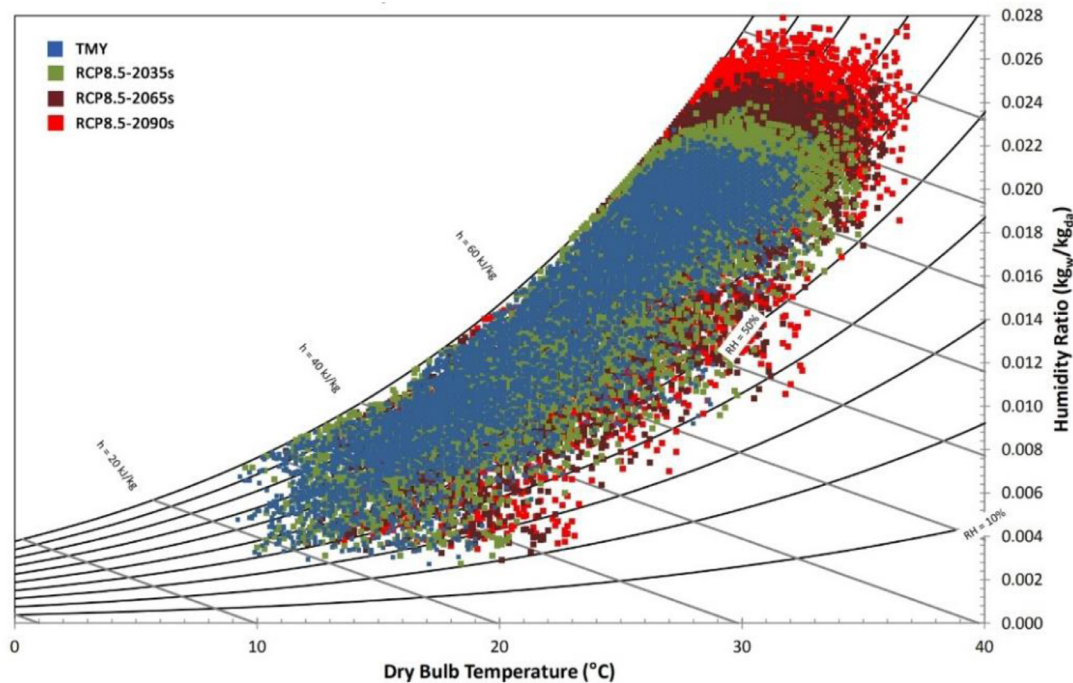


Fig. 3. Psychrometric chart of hourly weather data in the 2035s, 2065s, 2090s under the RCP8.5 and TMY scenarios.

2.3. Building simulation model setting

There are various types of residential buildings in Hong Kong. However, almost half of the total population live in public rental housing (PRH) due to the affordable price and governmental incentives [50]. Most of the PRH buildings are 10–30 storeys with a uniform and symmetric floor plan and are managed by the Housing Authority [51]. The floor plan of the Concord type PRH building, adopted in most of the latest PRH developments in Hong Kong, is given in Fig. 4. Due to the variations in physical building param-

eters (e.g., dimensions, materials, and glazing ratio) between different building types, e.g., public and private housing buildings, discrepancies of the energy demand between different building types could be identified. However, the aim of this study is rather to evaluate the impacts of climate change on the typical residential buildings using the newly developed future weather data, and not to conduct a detailed performance analysis of the building stock for the whole city. Found in around 70% of all PRH estates built after 2000, the Concord and Harmony PRH building types with cruciform floor plans are currently the dominant PRH building types.

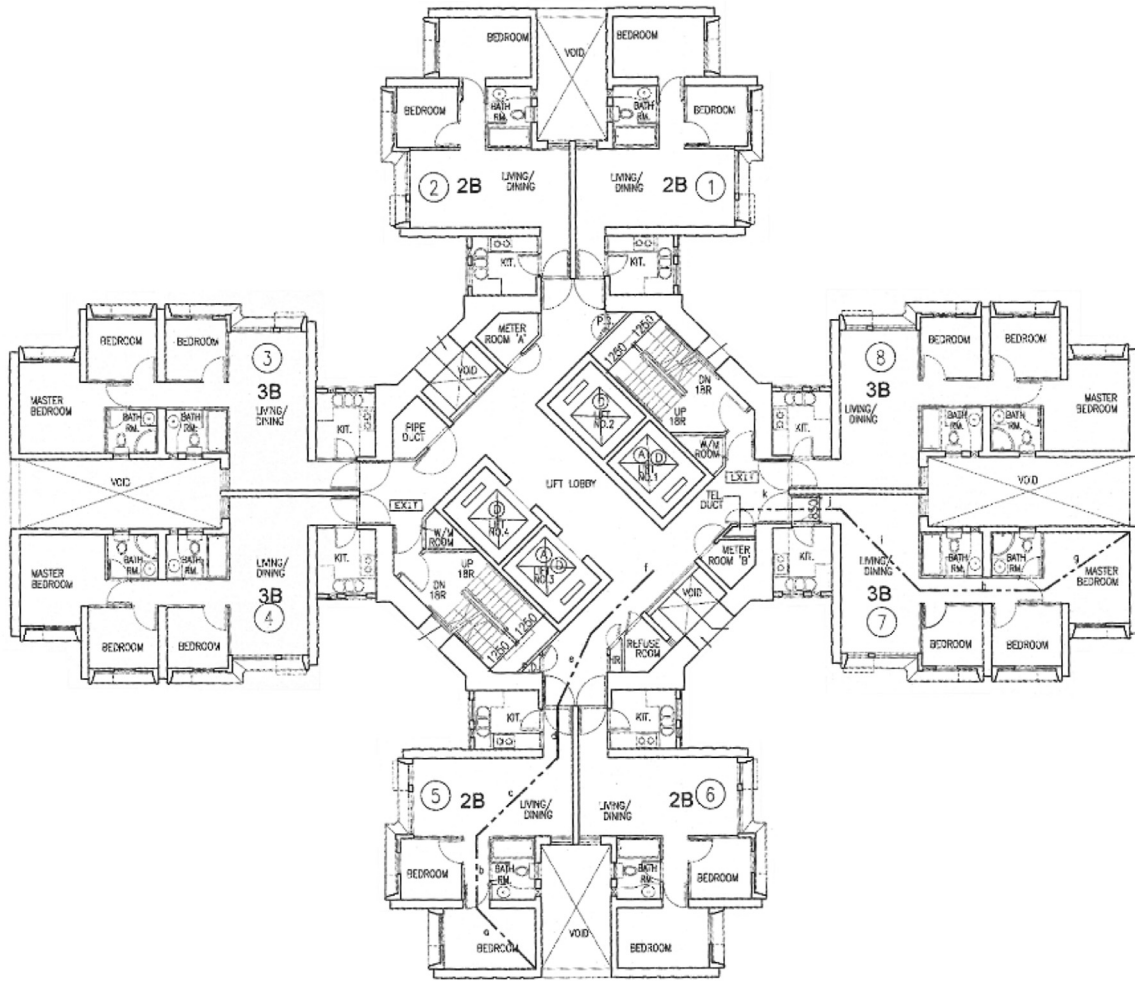


Fig. 4. Floor plan of Concord type Public Rental House in Hong Kong.

They also serve as the prototype for other newly developed PRH estates in Hong Kong, and will continue to be built across the city by the government in the future [52,53]. Therefore, the more prevalent Concord PRH building type is chosen as the representative case to indicate the potential impacts of climate change.

A dynamic building simulation tool, EnergyPlus, is applied for building simulation under the different future weather scenarios. Developed and supported by the U.S. Department of Energy, this tool has been widely used and extensively tested and validated in dynamic building simulations [54]. The building simulation model is set up with the DesignBuilder V5 interface and has already been used in previous works by the authors, e.g. [55,56]. More details of the inputs of building parameters, occupant schedules, and internal loads are appropriately documented in the literature [56–59]. Some key information on building physical parameters are presented in Table 2. The U-values of walls, roofs and glazing are calculated within DesignBuilder by constructing the building envelope materials with reference to the Baseline Building of the BEAM plus manual [32] and previous studies. It is also assumed that there are no interventions during the life cycle of the PRH building, keeping these building physical parameters as they are at the moment.

Due to the local PRH occupant behavior, the occupant-controlled natural ventilation is an important strategy to maintain indoor thermal comfort in the summer seasons [55]. The common usage behavior of air-conditioning in Hong Kong for PRH residents

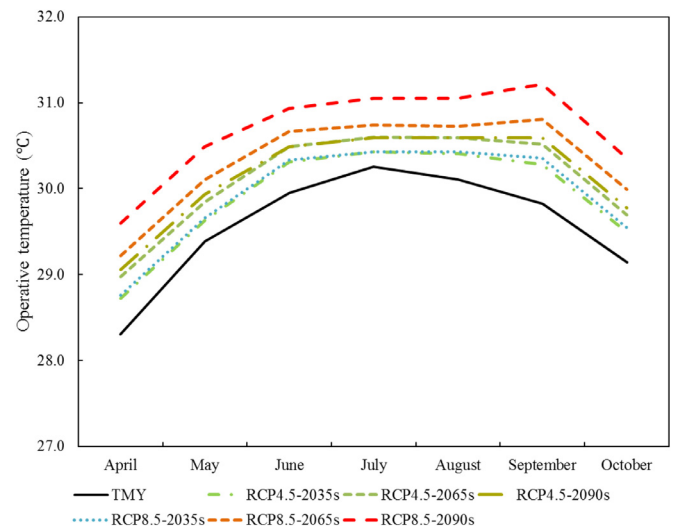


Fig. 5. The ASHRAE 80% upper acceptable adaptive thermal comfort for different climate scenarios in three periods.

is a hybrid ventilation mode, whereby the air-conditioner is used and windows are closed only when the indoor thermal comfort

Table 2
Building physical parameters for the models used in the simulations.

Physical parameters	Building type Concord type PRH
Total occupied floor area (m ²)	325.1
Cooled area (i.e. living room, bedroom) (m ²)	256.8
U-value of external wall (W m ⁻² K ⁻¹)	2.75
Window to external wall ratio	0.148
Floor height (m)	2.75
Wall solar absorptance	0.58
Window Open Area Ratio	0.30
U-value of roof (W m ⁻² K ⁻¹)	0.58
U-value of internal partition (W m ⁻² K ⁻¹)	2.86
U-value of floor slab (W m ⁻² K ⁻¹)	2.48
U-value of glazing (W m ⁻² K ⁻¹)	5.75
Solar heat gain coefficient of glazing	0.6

is intolerable [23]. It means that ventilation through windows is still a major strategy for cooling the indoor environment, while the operation of air-conditioner is a supplementary solution only when the indoor temperature exceeds the occupants' thermal comfort threshold. The window-opening schedule is controlled by the changeover mixed-mode in this study to prevent the simultaneous natural ventilation and heating, ventilation and air conditioning (HVAC) system cooling operation [60]. In this study, the simulations are first conducted under free-running conditions to isolate the effects of natural ventilation on the indoor thermal comfort. The mixed-mode is then applied to evaluate the cooling demand under the air-conditioned indoor environment.

The Airflow Network model in EnergyPlus is used to model the natural infiltration driven by the outdoor wind pressure and air flow through cracks and window/doors opening. It can be used to achieve the detailed simulation for the mixed-mode buildings. When the windows are closed, the cracks and gaps in the fabric of the building envelope provide the routes for air infiltration. The air infiltration rate in the natural ventilation or mixed-mode is governed by the airtightness of a building, the distribution of leakage openings, and the magnitude of pressures acting at each opening. In this study, the vertical window opening on the external wall is set to a constant air flow exponent of 0.60 to represent an empirically poor level of airtightness, as suggested by the Numerical Data for Air Infiltration & Natural Ventilation Calculations [61]. The TMY and the morphed future hourly weather data are adopted as the weather inputs. The cooling season of air-conditioning is commonly set from April to October in Hong Kong based on the local green building recommendations of BEAM Plus [32].

2.4. Thermal comfort criteria

The thermal comfort criterion to determine whether the indoor thermal conditions are comfortable, and therefore the need to operate air-conditioning, is an important consideration when simulating a mixed-mode building. In naturally ventilated or mixed-mode buildings, the traditional indoor thermal comfort standard, predicted mean vote (PMV), is less suitable due to the psychological thermal expectations [62,63]. The adaptive comfort standard (ACS) model links the indoor thermal comfort criteria with the outdoor temperature, and thus results in a greater tolerance and a wider range of acceptability of the occupants' comfort [64]. In the hot and humid subtropical climate, Luo et al. [65] found that the ACS model are more applicable to mixed-mode buildings than the steady-state comfort model. In this study, the widely adopted and recognized ASHRAE Standard 55-2017 [66] is applied in the mixed-mode residential building model. This ACS approach addresses the thermal adapting behaviors by introducing an equation of the mean outdoor air temperature of each calendar month

(T_{ao}) in relation to the upper 80% acceptability limits of indoor operative temperature ($T_{o,up80}$) as follows:

$$T_{o,up80} = 0.31T_{ao} + 21.3 \quad (4)$$

The future climate conditions are also within the range of outdoor thermal criteria set in the ASHRAE Standard 55, in which the ACS model is applicable for prevailing mean outdoor air temperatures between 10 °C and 33.5 °C.

With reference to Fig. 5, the adaptive model assumes that the occupants' upper thermal comfort threshold will gradually adapt to the outdoor climate. Although global warming is inevitable in Hong Kong, this adaptive model could provide a slight relief for the potential increase of energy consumption in the PRH buildings. To calculate the realistic cooling energy demand based on the operative temperature threshold in each thermal zone in EnergyPlus, the indoor operative temperature is selected for sizing the air-conditioning cooling load. When the indoor operative temperature exceeds the thermal comfort threshold $T_{o,up80}$, the HVAC system is operated and the windows are assumed to be closed manually. Hence, the discomfort hours, i.e., cooling hours, can be defined as the hours with the indoor operative temperature above $T_{o,up80}$.

3. Results and discussion

3.1. Impacts of future climate on the indoor thermal comfort

The impacts of climate change on indoor thermal comfort are first described by the cumulative percentage of time when indoor air temperature (Fig. 6)/ relative humidity (Fig. 7) of the PRH exceeds a certain temperature/ relative humidity value. During the cooling season, the median indoor air temperature increases from 27.5 °C for TMY to 28.6 °C for RCP4.5-2030s, 28.7 °C for RCP8.5-2035s, 29.2 °C for RCP4.5-2065s, 29.4 °C for RCP4.5-2090s, 30.0 °C for RCP8.5-2065s, and 30.5 °C for RCP8.5-2090s. The cumulative distribution also shows that the proportion of time when indoor air temperature exceeds 32.8 °C increases from 1.2% in TMY to 9.5% in RCP4.5-2090s and 24.2% in RCP8.5-2090s. Upon considering relative humidity, the future percentile with range from 40% to 90% generally decreases for all scenarios, while the hours with relative humidity above 90% have some small increments. After adopting the ACS, the cooling hours, i.e., the discomfort hours, and their percentage are calculated and displayed in Table 3. Compared to the small number of cooling hours in TMY, it can be seen that the discomfort hours in April, May and October have the most considerable relative increase, while the annual total discomfort hours increase from 1128 (21.9%) in TMY to 1849 (36.0%) in RCP4.5-2090s and 2591 (50.4%) in RCP8.5-2090s. Referring to the cumulative time of air temperature in Fig. 6 and discomfort hours in Table 3, there are negligible differences between the two RCP scenarios in 2035s and between the periods from 2065s to 2090s in RCP4.5 scenario.

3.2. Impacts of future climate on the building energy demand

The computed results for each month under TMY and future climate scenarios are plotted in Fig. 8. An appreciable growth of building cooling demand is evident in the different future scenarios. The higher relative increase of cooling load in April, May and October may be explained by the higher relative increase of discomfort hours as discussed earlier in Section 3.1. Since there are few discomfort hours under the present TMY in the transition season, the relative increase of energy demand in the transition season caused by the future climate change are larger than those months near midsummer, e.g., the cooling load in April is expected to increase dramatically from 0.53 kWh/m² for TMY to 7.23 kWh/m² for RCP8.5-2090s (+1264%), while the cooling load

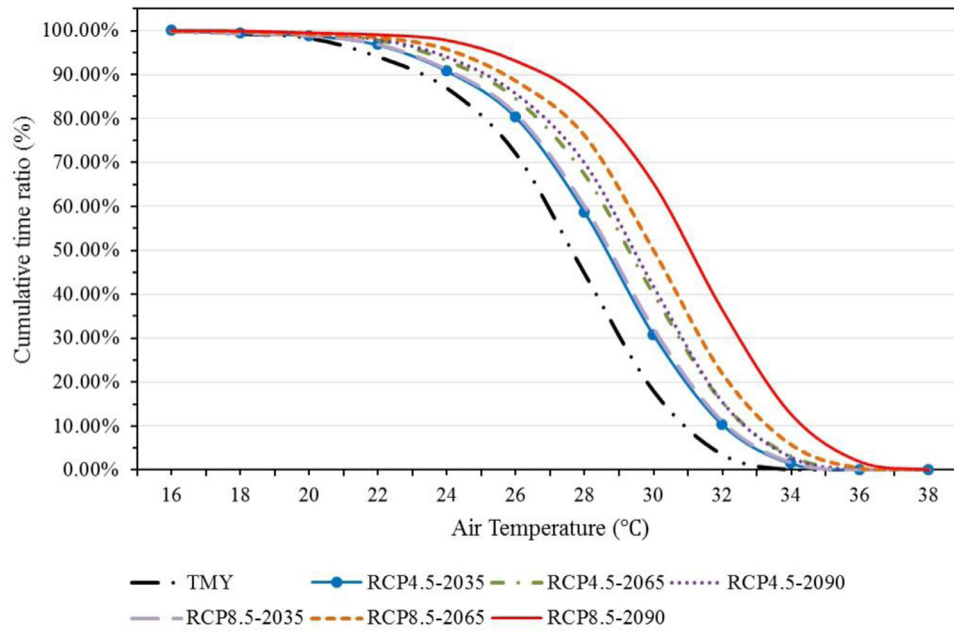


Fig. 6. Cumulative percentage of time above certain air temperature in bedrooms from April to October for different climate scenarios.

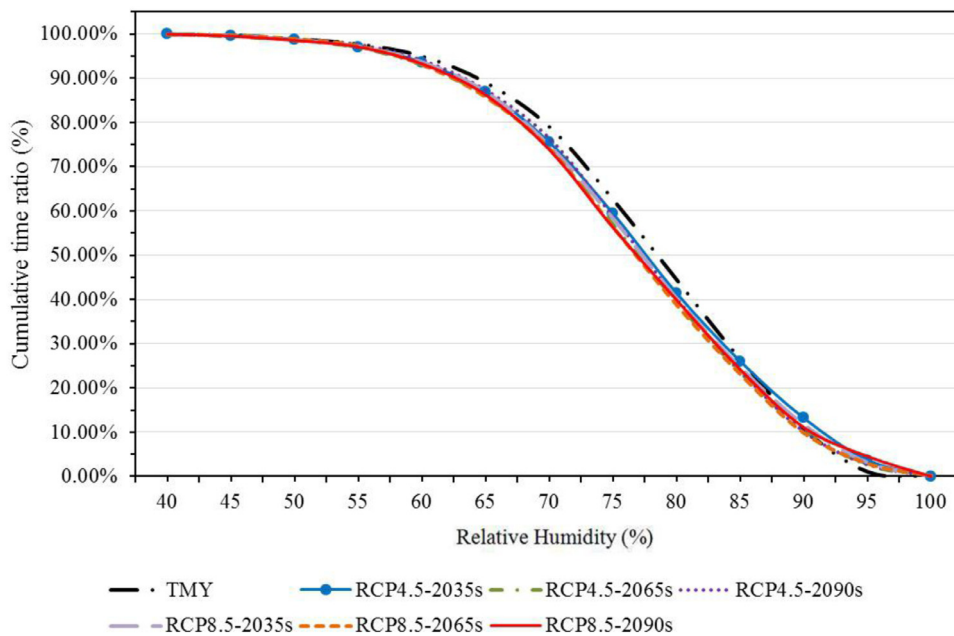


Fig. 7. Cumulative percentage of time above certain relative humidity in bedrooms from April to October for different climate scenarios.

Table 3
Discomfort hours and their percentage of each month under the different climate scenario using ASHRAE Comfort Model 55.

Month	TMY	RCP4.5			RCP8.5		
	1979–2003	2035s	2065s	2090s	2035s	2065s	2090s
April	29(4.0%)	87(12.1%)	109(15.1%)	117(16.3%)	84(11.7%)	139(19.3%)	184(25.6%)
May	97(13.0%)	157(21.1%)	214(28.8%)	220(29.6%)	162(21.8%)	272(36.6%)	324(43.5%)
June	221(30.7%)	285(39.6%)	313(43.5%)	300(41.7%)	285(39.6%)	335(46.5%)	368(51.1%)
July	297(39.9%)	344(46.2%)	387(52.0%)	362(48.7%)	350(47.0%)	408(54.8%)	469(63.0%)
August	265(35.6%)	337(45.3%)	393(52.8%)	379(50.9%)	337(45.3%)	410(55.1%)	449(60.3%)
September	162(22.5%)	249(34.6%)	323(44.9%)	336(46.7%)	265(36.8%)	405(56.3%)	482(66.9%)
October	57(7.7%)	90(12.1%)	136(18.3%)	135(18.1%)	112(15.1%)	192(25.8%)	315(42.3%)
Total	1128(21.9%)	1549(30.2%)	1875(36.5%)	1849(36.0%)	1595(31.1%)	2161(42.1%)	2591(50.4%)

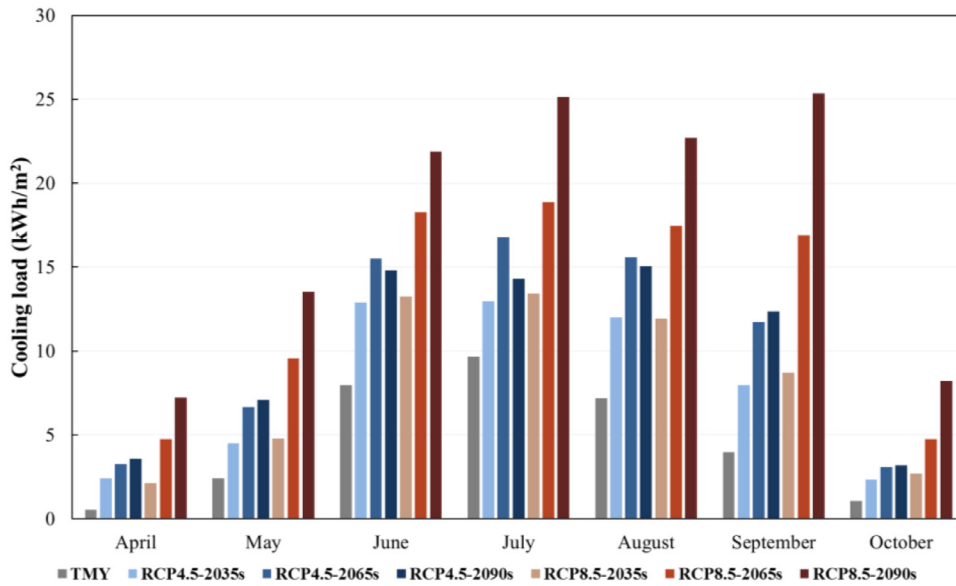


Fig. 8. The change in monthly cooling load of typical PRH buildings under the different climate scenarios.

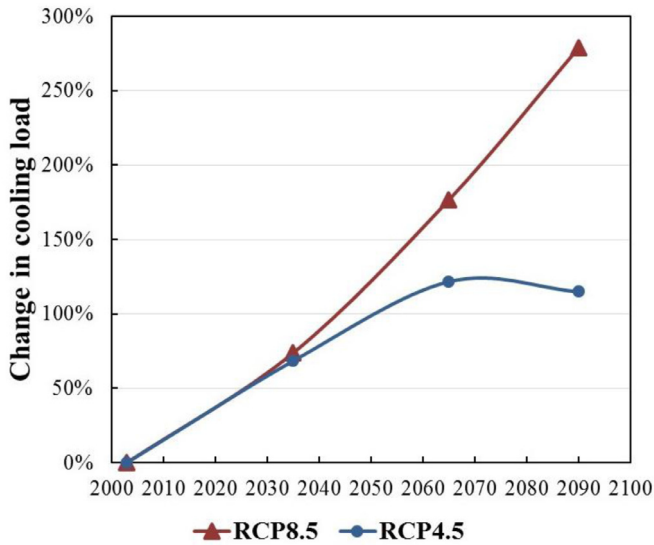


Fig. 9. The percentage change in annual cooling load of typical PRH buildings under climate scenarios RCP4.5 and RCP8.5.

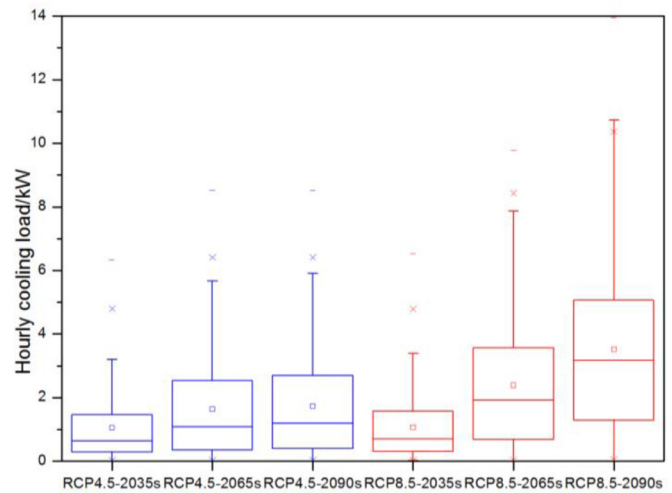


Fig. 10. The hourly cooling load in the increased discomfort hours of the future climate scenarios.

in July is expected to increase from 9.66 kWh/m² for TMY to 25.12 kWh/m² for RCP8.5–2090s (+160%). Another notable feature of the monthly cooling load is that the highest cooling loads will still be required in the months from June to September under the future scenarios. When comparing RCP4.5–2065s with RCP4.5–2090s, higher monthly cooling loads can be found in June, July, and August for the former. This discrepancy corresponds to the slightly higher number of the discomfort hours in those three months for RCP4.5–2065s compared to RCP4.5–2090s, as shown in Table 3. This monthly distribution pattern follows the same trend as the previous survey about the overall energy consumption in residential units in Hong Kong [30].

Compared with the cooling load in the building model with TMY weather data, the simulated results of the percentage change for annual building cooling load under the two selected RCP scenarios are also presented in Fig. 9. An appreciable divergence in the

building energy demand can be observed after the near-term period (2035s). This trend of yearly cooling load generally followed the tendency of yearly outdoor air temperature change as presented in Fig. 1. For the RCP4.5 scenario, the relative change of building cooling load will reach to the peak value about 121.61% by 2065s, after which the cooling load decreases slightly at the end of this century. This is because total cooling hours, and thus the cooling loads, in RCP4.5–2065s are larger than in RCP4.5–2090s, particular for the months June, July, and August, as shown in Fig. 8 and Table 3. By contrast, under the RCP8.5 scenario, the building cooling demand at the end of this century will substantially increase by about 278.80% of the present TMY scenario, almost tripling the TMY cooling load. Furthermore, the increase of cumulative energy demand is not proportional to the percentage increase in cooling hours shown in Table 3. This result may be explained by the synergy effect of the increase in both the number of cooling hours and the absolute air temperature increase in each hour. On the one hand, the increase in the number of cooling hours means that the

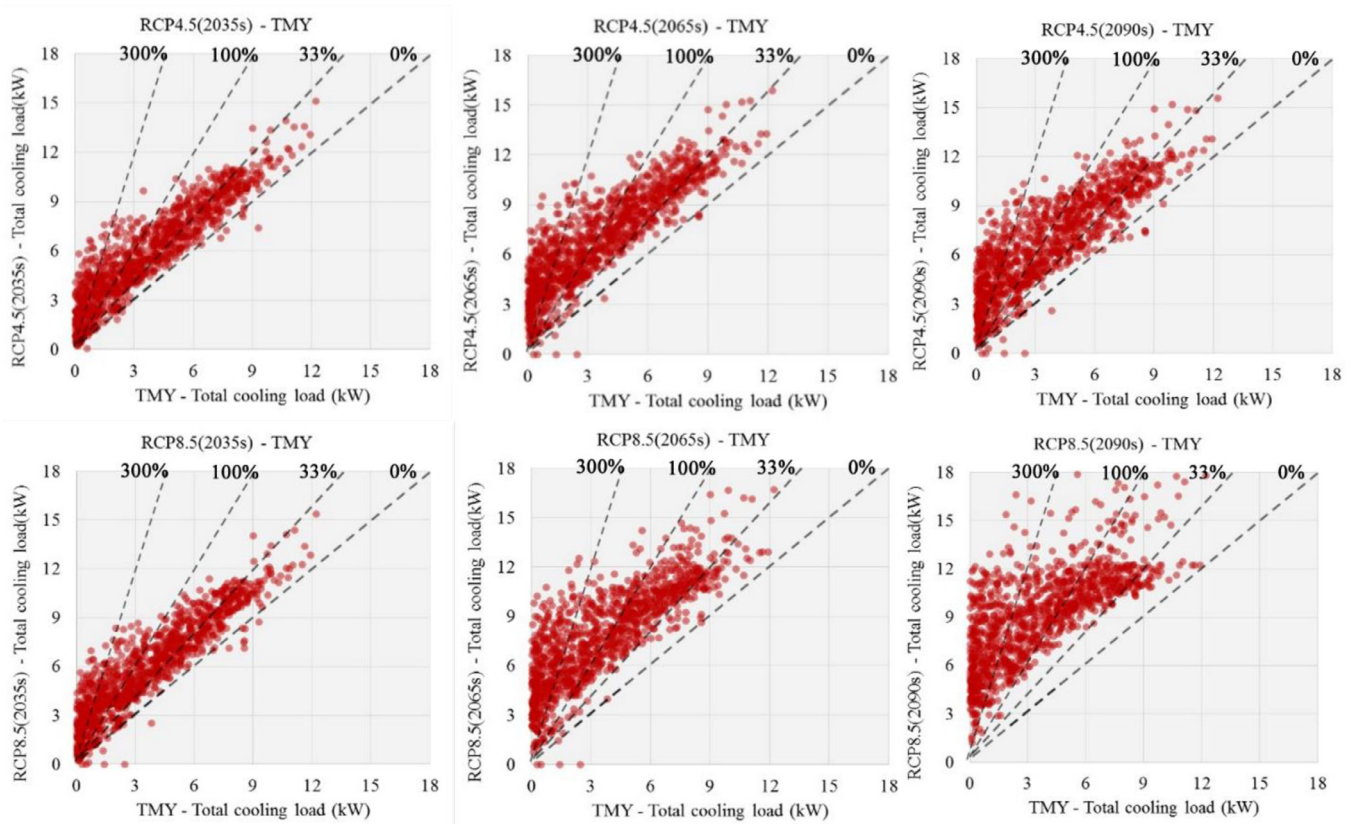


Fig. 11. Relation between the hourly cooling load from TMY and the future climate scenarios in the original cooling hours.

occupants are more likely to use air-conditioning in the future, resulting in the increase of cooling load. This is the so-called 'switching behaviour' of the occupants when indoor operative temperatures exceed the thermal comfort threshold. On the other hand, the exacerbated cooling demands are caused by the higher air temperature in the original cooling hours. Discrepancies of the increased degree of cooling load between different RCP scenarios can be further confirmed by this synergy effect, which is discussed in the following paragraphs.

In the case of hourly cooling load, the increase of cumulative cooling demands can be attributable to the cooling demands in the increased discomfort time and the increased degree of cooling load in the original cooling hours. The hourly cooling load in the increased discomfort hours of the future climate scenarios is shown in Fig. 10. The median cooling load per hour is expected to increase by 1.3 kW and 3.2 kW per hour for RCP4.5 and RCP8.5 in 2090s, while the maximum of the increased cooling load can even reach above 6 kW and 10 kW per hour for RCP4.5 and RCP8.5 in 2090s. Under those circumstances in the future, the usage time of air conditioning can unavoidably be prolonged and the capacity of HVAC systems need to be improved to meet the significantly increased degree of cooling demands. Compared with the discrepancies of annual cooling load between the different climate scenarios, boxplots of the hourly cooling loads for the different scenarios confirm their divergences.

With regard to the percentage change of the hourly cooling load in the original cooling hours of TMY, taking the hourly cooling load of TMY as the reference value in the calculation of the percentage changes, the relationship between TMY and the future climate scenarios are shown in Fig. 11. After calculating the counts of hours

with different ranges of relative change, the distribution of cooling hours with the different range of relative change is summarized in Table 4. Results indicate that the number of hours within the change range from 33% to 100% is the dominant percentage change from 2035s to 2090s for both two scenarios, except that hours with relative change more than 300% are the major part in RCP8.5–2090s. This means that the higher magnitude of cooling demands becomes more frequent over time and the majority of percentage change of cooling load are larger than 100% after 2065s. In terms of the absolute change, the mean value of cooling load per hour is increased by 2.05 kW and 2.19 kW in 2035s, 3.26 kW and 4.12 kW in 2065s, and 3.03 kW and 5.42 kW in 2090s, for RCP4.5 and RCP8.5, respectively. Those results reconfirm that the noticeable divergence will be occurred in the long-term period between the different RCP scenarios.

Considering the change in maximum cooling load, the results depict that there are no significant fluctuations for RCP4.5 with a relative change from 23.60% to 29.79%. As for RCP8.5, the percentage change of cooling load increases from 25.66% in 2035s to 54.25% in 2090s. However, when compared to the percentage change in overall cooling load, the percentage change in maximum cooling load is at a considerably lower level. Under the future climate scenarios, especially in RCP8.5–2090s, one can also note from Fig. 11 that the maximum of cooling load rarely exceeds 13 kW per hour. Those features regarding the change of maximum cooling load may imply that there is an underestimated effect on the maximum cooling loads. This can be partly explained by the limitations of the morphing method, as there is an inherent assumption that the future weather patterns will be identical with the baseline TMY weather file, which excludes the extreme weather

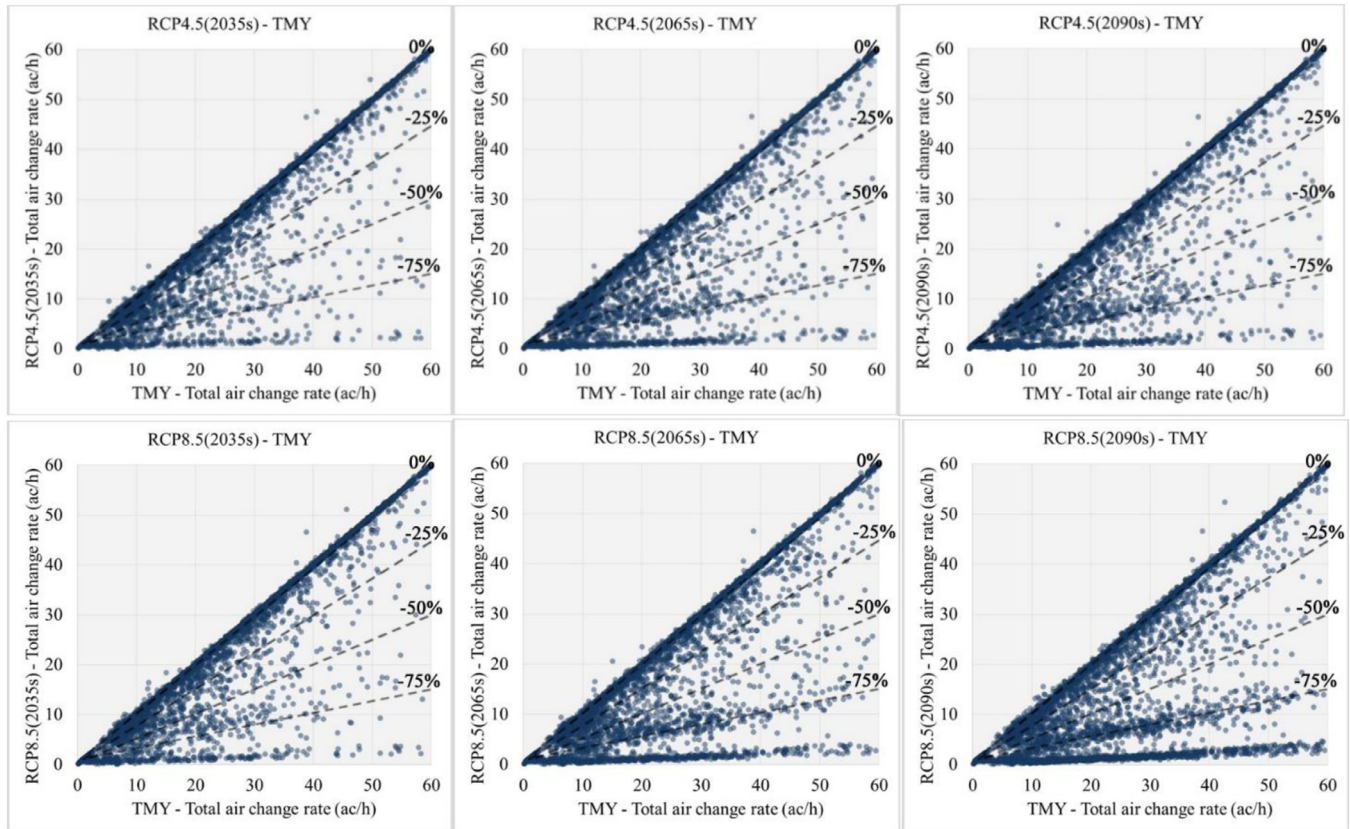


Fig. 12. Relation between hourly air change rate from TMY and the future climate scenarios.

Table 4

The relative change of cooling load between TMY and the future climate scenarios in the original cooling hours.

Scenarios	Hours in 0%–33%	Hours in 33%–100%	Hours in 100%–300%	Hours in $\geq 300\%$	Mean value of absolute change per hour (kW)	Maximum cooling load (kW) and the relative change (%)
RCP4.5(2035s)	292	405	214	196	2.05	15.11 kW, 23.60%
RCP4.5(2065s)	116	440	263	291	3.26	15.87 kW, 29.79%
RCP4.5(2090s)	176	404	238	299	3.03	15.56 kW, 27.27%
RCP8.5(2035s)	272	392	237	202	2.19	15.37 kW, 25.66%
RCP8.5(2065s)	69	407	304	335	4.12	16.71 kW, 36.71%
RCP8.5(2090s)	45	300	375	398	5.42	18.86 kW, 54.25%

conditions [67]. Therefore, the future peak cooling demand under more frequent events of extreme weather conditions such as heat wave will likely exceed the estimations in this paper.

3.3. Impacts of future climate on the air change rate

Natural ventilation in mixed-mode buildings is also considerably affected by the future increasing temperatures. Taking the air change rate with existing TMY file as the baseline, Fig. 12 presents the relationship between the percentage changes in air change rates between TMY and the future scenarios. The absolute and relative change for each hour is shown in Table 5. The mean absolute value of the reduction in air change rate per hour is increased from 2.30 ac/h to 3.55 ac/h, representing -11.14% and -16.14% of relative change under RCP4.5 scenario from 2030s to 2090s, and increased from 2.47 ac/h to 8.06 ac/h under RCP8.5 scenario, representing -11.81% and -32.28% of relative change. As can be seen, there is a substantial increase in the number of points below the line of -75% for both future scenarios, and this trend of increasing dots becomes more evident over time. From 2035s to 2090s, the

number of hours with change range from 0% to -25% passes from 4291 to 3968 under RCP4.5 scenario and from 4238 to 2982 under RCP8.5 scenario respectively, while the counts of hours with relative change from -75% to -100% are dramatically increased from 270 to 420 for RCP4.5 and from 296 to 1168 for RCP8.5. Those hours with relative reduction of air change rate beyond 75% mainly occurred during hours with increased cooling load in the future, corresponding to the period of when the use of natural ventilation is replaced by air conditioning operation in the mixed-mode residential building. By contrast, the majority of hours still fall on or next to the line of 0% for each scenario. This is because the amount of comfort hours from April to October is still larger than the numbers of discomfort hours except in the RCP8.5–2090s, as shown in the Table 3. During the comfort hours of mixed-mode buildings, it is assumed that the natural ventilation through windows remains at the major cooling strategy. If the natural ventilation is not changed into mechanical ventilation in the comfort hours from TMY to the future scenarios, the air change rate under the natural ventilation environment should be kept almost the same.

Table 5
Relative change of hourly air change rate between TMY and the future climate scenarios.

Scenarios	Hours in 0%– – 25%	Hours in – 25%– – 50%	Hours in – 50%– – 75%	Hours in – 75%– – 100%	Relative average change per hour	Mean value of absolute change per hour (ac/h)
RCP4.5(2035s)	4291	291	236	270	–11.14%	2.30
RCP4.5(2065s)	3944	317	377	450	–16.41%	3.66
RCP4.5(2090s)	3968	307	393	420	–16.14%	3.55
RCP8.5(2035s)	4238	312	242	296	–11.81%	2.47
RCP8.5(2065s)	3586	343	487	627	–22.07%	5.22
RCP8.5(2090s)	2982	376	562	1168	–32.28%	8.06

Our findings support the findings from previous studies [8,68], which state a decline in the efficiency of natural ventilation during nighttime for residential buildings in the future. Their results revealed that, in the future, there will be a considerable reduction in natural ventilation between indoor and outdoor spaces due to the impacts of climate change, resulting in an increasing demand of fresh air supply through HVAC mechanical ventilation and a poor indoor environment quality. The warmer ambient temperature not only causes the increased risks of indoor overheating and the overloading of HVAC systems as discussed earlier, but also results in an increasing age of air and may lead to subsequent fresh air and indoor air quality (IAQ) issues for occupants [69,70]. Because the window-opening schedule is controlled by the changeover mixed-mode in the hybrid residential buildings, it is assumed that the windows are closed as long as the air-conditioner is operation. Since there are more cooling hours, i.e., the hours of closing windows and doors, in the future climate scenarios, the air change effectiveness is subsequently decreasing due to the closing of the window and the door. Thus, there is a great potential use of advanced ventilation systems, e.g., the displacement ventilation and underfloor air distribution system, in the future due to the increased demand in fresh air supply [71]. These types of ventilation systems can be effective for creating a better IAQ and comfortable environment by supplying fresh air and eliminating contamination without more ventilation load.

4. Conclusions

In this study, six sets of future hourly weather data have been constructed for subtropical Hong Kong by morphing the baseline climate, represented by the TMY weather data, with downscaled data from 24 GCMs in the CMIP5. With the help of building energy simulation tools, the newly developed future design weather data can be used by researchers, building energy engineers, and architects to study the impacts of future climate and discuss the potential mitigation/adaptation technologies at the building scale. By employing this newly developed future weather data, the future building energy demand in PRH buildings in Hong Kong is then evaluated for different RCP scenarios. To represent the acclimatization effects on occupant behavior under the changing climate conditions, the adaptive thermal comfort model has been adopted in building operating in hybrid/mixed-mode ventilation. Although we have taken into account the acclimatization effects and the conservative use of air-conditioning in mixed-mode buildings, a dramatic increase in the cooling load and reduction in air change rate is still inevitable. By the end of this century, our findings indicate that the annual cooling load will increase by 114.90% and 278.80% and the air change rate will reduce by 16.14% and 32.28% per hour for RCP4.5 and RCP8.5 scenarios, respectively. Moreover, the mean value of cooling load per hour is increased by 3.03 kW and 5.42 kW and the mean value of air change rate is reduced by 3.55 ac/h and 8.06 ac/h for RCP4.5 and RCP8.5, respectively.

Note that the almost three-fold increase in annual cooling load for RCP8.5 may be attributable to the synergistic effects of both the increased amount of time when occupants use air-conditioning (i.e. the increase in number of cooling hours) and the higher cooling load per original cooling hour with increased temperatures.

To combat the adverse effects of future climate change, the increased cooling hours and cooling loads could be significantly mitigated by adopting the passive retrofitting strategies e.g., wall insulation, glazing materials, external shading, cooling roof and wall, for those PRH buildings. Also, more advanced ventilation systems, such as the displacement ventilation and underfloor air distribution system, are more required in the future due to the increasing needs of indoor fresh air supply. Future works for discussing the effectiveness of these adaptation strategies still need to be done. Other limitations of the current study are as follows: as this study only takes one case study into account, i.e., the typical PRH building type, it is unable to quantify the uncertainties caused by different building design features, such as the window-to-wall ratio, building orientation, wall insulation, glazing material, and thermal mass. Therefore, results presented in the study only serve as the reference values for Concord type PRH buildings and other similar building types, instead of the mixture of total building stock. Secondly, although the annual and monthly results could be comprehensively predicted by using the morphed data, this approach may not fully reflect the future extreme weather conditions and the urban microclimate, and is thus limited in terms of the evaluation of the impacts on building peak cooling loads in the future. When more sophisticated RCMs with finer spatial and temporal resolutions become available locally, the energy robustness of buildings under the extreme boundary conditions could be better discussed.

Declaration of Competing Interest

The authors declare no conflict of interest.

CRediT authorship contribution statement

Sheng Liu: Conceptualization, Investigation, Methodology, Visualization, Writing - original draft. **Yu Ting Kwok:** Conceptualization, Investigation, Writing - review & editing. **Kevin Ka-Lun Lau:** Conceptualization, Methodology, Supervision, Funding acquisition. **Hong Wai Tong:** Data curation, Resources. **Pak Wai Chan:** Data curation, Resources. **Edward NG:** Supervision, Funding acquisition.

Acknowledgments

This work is fully supported by the Vice-Chancellor's Discretionary Fund of the [Chinese University of Hong Kong](#) and the Research Impact Fund (Ref: R4046-18F) of Research Grant Council, Hong Kong.

Appendix

Table A1

List of CMIP5 general circulation models applied in this study.

model designation	modeling group	Group Acroynm	Scenarios
ACCESS1-0	Commonwealth Scientific and Industrial Research Organization	CSIRO	RCP4.5, RCP8.5
BCC-CSM1-1	Beijing Climate Center, China Meteorological Administration	BCC	RCP4.5, RCP8.5, RCP2.6, RCP6.0
BNU-ESM	College of Global Change and Earth System Science, Beijing Normal University	GCESS,BNU	RCP4.5, RCP8.5, RCP2.6
CanESM2	Canadian centre for Climate Modeling and Analysis	CCCma	RCP4.5, RCP8.5, RCP2.6
cnrm-cm5	centre national de recherches météorologiques	CNRM	RCP4.5, RCP8.5, RCP2.6
CSIRO-Mk3-6-0	Commonwealth Scientific and Industrial Research Organization	CSIRO	RCP4.5, RCP8.5, RCP2.6, RCP6.0
GFDL-ESM2G	NOAA Geophysical Fluid Dynamics Laboratory	NOAA GFDL	RCP4.5, RCP8.5, RCP6.0
GFDL-ESM2M	NOAA Geophysical Fluid Dynamics Laboratory	NOAA GFDL	RCP4.5, RCP8.5, RCP6.0
HadGEM2-CC	Met-Office Hadley centre	MOHC	RCP4.5, RCP8.5
INM-CM4	Institute for Numerical Mathematics	INM	RCP4.5, RCP8.5
IPSL-CM5A-LR	Institut Pierre-Simon Laplace	IPSL	RCP4.5, RCP8.5, RCP2.6, RCP6.0
IPSL-CM5A-MR	Institut Pierre-Simon Laplace	IPSL	RCP4.5, RCP8.5, RCP2.6, RCP6.0
IPSL-CM5B-LR	Institut Pierre-Simon Laplace	IPSL	RCP4.5, RCP8.5
MIROC5	Japan Agency for Marine-Earth Science and Technology, Atmosphere and Ocean Research Institute, The University of Tokyo	MIROC	RCP4.5, RCP8.5, RCP2.6, RCP6.0
MIROC-ESM	Japan Agency for Marine-Earth Science and Technology, Atmosphere and Ocean Research Institute, The University of Tokyo	MIROC	RCP4.5, RCP8.5
MIROC-ESM-CHEM	Japan Agency for Marine-Earth Science and Technology, Atmosphere and Ocean Research Institute, The University of Tokyo	MIROC	RCP4.5, RCP8.5, RCP2.6, RCP6.0
MPI-ESM-LR	Max-Planck-Institut für Meteorologie	MPI	RCP4.5, RCP8.5, RCP2.6
MRI-CGCM	Meteorological Research Institute	MRI	RCP4.5, RCP8.5, RCP6.0
Nor-ESM1-M	Norwegian Climate centre	NCC	RCP4.5, RCP8.5, RCP2.6, RCP6.0
MPI-ESM-MR	Max-Planck-Institut für Meteorologie	MPI	RCP4.5, RCP8.5, RCP2.6
ACCESS1-3	Commonwealth Scientific and Industrial Research Organization	CSIRO	RCP4.5, RCP8.5
BCC-CSM1-1-m	Beijing Climate Center, China Meteorological Administration	BCC	RCP4.5, RCP8.5, RCP2.6, RCP6.0
CMCC-CMS	Centro Euro-Mediterraneanoper I Cambiamenti Climatici	CMCC	RCP4.5, RCP8.5
CMCC-CM	Centro Euro-Mediterraneanoper I Cambiamenti Climatici	CMCC	RCP4.5, RCP8.5

Table A2

The mean, standard deviation, and range of temperature anomaly in each decade under the different RCP scenarios.

Period	RCP2.6			RCP4.5			RCP6.0			RCP8.5		
	Mean	σ	Range	Mean	σ	Range	Mean	σ	Range	Mean	Σ	Range
2000–2009	0.24	0.27	−0.19–0.85	0.29	0.25	−0.08–0.97	0.40	0.10	0.26–0.61	0.42	0.32	−0.16–1.27
2010–2019	0.54	0.17	0.20–0.80	0.53	0.23	0.21–1.36	0.50	0.15	0.25–0.79	0.58	0.25	0.28–1.09
2020–2029	0.80	0.21	0.43–1.16	0.79	0.24	0.27–1.48	0.70	0.18	0.41–0.98	0.91	0.27	0.52–1.68
2030–2039	1.04	0.22	0.67–1.42	1.10	0.38	0.40–2.22	0.74	0.17	0.51–1.08	1.17	0.28	0.66–1.82
2040–2049	1.24	0.32	0.72–1.67	1.36	0.31	0.73–2.11	1.01	0.24	0.64–1.41	1.58	0.39	0.89–2.47
2050–2059	1.32	0.27	0.90–1.71	1.62	0.43	0.75–2.72	1.20	0.25	0.86–1.69	2.11	0.53	1.14–3.30
2060–2069	1.35	0.33	0.86–1.86	1.82	0.47	1.08–2.85	1.46	0.30	1.01–2.04	2.57	0.57	1.60–3.83
2070–2079	1.28	0.30	0.81–1.72	1.99	0.51	1.15–3.09	1.87	0.32	1.40–2.42	3.03	0.67	1.86–4.33
2080–2089	1.28	0.39	0.77–2.00	2.06	0.52	1.26–3.52	2.11	0.45	1.55–2.77	3.51	0.77	2.16–5.05
2090–2099	1.18	0.28	0.83–1.72	2.06	0.56	1.10–3.26	2.35	0.44	1.74–2.90	4.03	0.86	2.80–5.48

References

- [1] IPCC, Climate Change 2014: Synthesis Report. Contribution of Working Groups I, II and III to the Fifth Assessment Report of the Intergovernmental Panel on Climate Change, IPCC, Geneva, Switzerland, 2014.
- [2] IPCC, IPCC special report on emissions scenarios. Intergovernmental Panel on Climate Change, 2000.
- [3] IPCC, Climate Change 2007: Synthesis Report. Contribution of Working Groups I, II and III to the Fourth Assessment Report of the Intergovernmental Panel on Climate Change, IPCC, Geneva, Switzerland, 2007.
- [4] IPCC, IPCC Fifth Assessment Report (AR5) now underway. Update on Scenario Development: from SRES to RCPs, 2010.
- [5] R.H. Moss, J.A. Edmonds, K.A. Hibbard, M.R. Manning, S.K. Rose, D.P. van Vuuren, et al., The next generation of scenarios for climate change research and assessment, *Nature* 463 (2010) 747–756, doi:10.1038/nature08823.
- [6] R. Lapsa, E. Bozonnet, P. Salagnac, M. Abadie, Optimized design of low-rise commercial buildings under various climates - Energy performance and passive cooling strategies, *Build. Environ.* 132 (2018) 83–95, doi:10.1016/j.buildenv.2018.01.029.
- [7] H.L. Macintyre, C. Heaviside, Potential benefit of cool roofs in reducing heat-related mortality during heatwaves in a European city, *Environ. Int.* 127 (2019) 430–441, doi:10.1016/j.envint.2019.02.065.
- [8] H.J. Wang, Q.Y. Chen, Impact of climate change heating and cooling energy use in buildings in the United States, *Energy Build.* 82 (2014) 428–436, doi:10.1016/j.enbuild.2014.07.034.
- [9] M. Santamouris, On the energy impact of urban heat island and global warming on buildings, *Energy Build.* 82 (2014) 100–113, doi:10.1016/j.enbuild.2014.07.022.
- [10] M. Santamouris, Cooling the buildings - past, present and future, *Energy Build.* 128 (2016) 617–638, doi:10.1016/j.enbuild.2016.07.034.
- [11] M. Isaac, D.P. van Vuuren, Modeling global residential sector energy demand for heating and air conditioning in the context of climate change, *Energy Policy* 37 (2009) 507–521, doi:10.1016/j.enpol.2008.09.051.
- [12] D.H.W. Li, L. Yang, J.C. Lam, Impact of climate change on energy use in the built environment in different climate zones - a review, *Energy* 42 (2012) 103–112, doi:10.1016/j.energy.2012.03.044.

- [13] J.H. Eto, On using degree-days to account for the effects of weather on annual energy use in office buildings, *Energy Build.* 12 (1988) 113–127, doi:10.1016/0378-7788(88)90073-4.
- [14] S. Bhartendu, S.J. Cohen, Impact of CO₂-induced climate change on residential heating and cooling energy requirements in Ontario, Canada, *Energy Build.* 10 (1987) 99–108, doi:10.1016/0378-7788(87)90012-0.
- [15] Z.J. Zhai, J.M. Helman, Implications of climate changes to building energy and design, *Sustain. Cities Soc.* 44 (2019) 511–519, doi:10.1016/j.scs.2018.10.043.
- [16] S.E. Belcher, J.N. Hacker, D.S. Powell, Constructing design weather data for future climates, *Build. Serv. Eng. Res. Technol.* 26 (2005) 49–61, doi:10.1191/0143624405bt112oa.
- [17] M.F. Jentsch, P.A.B. James, L. Bourikas, A.S. Bahaj, Transforming existing weather data for worldwide locations to enable energy and building performance simulation under future climates, *Renew. Energy* 55 (2013) 514–524, doi:10.1016/j.renene.2012.12.049.
- [18] P. Shen, N. Lior, Vulnerability to climate change impacts of present renewable energy systems designed for achieving net-zero energy buildings, *Energy* 114 (2016) 1288–1305, doi:10.1016/j.energy.2016.07.078.
- [19] P. Shen, Impacts of climate change on U.S. building energy use by using down-scaled hourly future weather data, *Energy Build.* 134 (2017) 61–70, doi:10.1016/j.enbuild.2016.09.028.
- [20] M.A. Triana, R. Lamberts, P. Sassi, Should we consider climate change for Brazilian social housing? Assessment of energy efficiency adaptation measures, *Energy Build.* 158 (2018) 1379–1392, doi:10.1016/j.enbuild.2017.11.003.
- [21] L. Pagliano, S. Carlucci, F. Causone, A. Moazami, G. Cattarin, Energy retrofit for a climate resilient child care centre, *Energy Build.* 127 (2016) 1117–1132, doi:10.1016/j.enbuild.2016.05.092.
- [22] G.R. Roshan, R. Oji, S. Attia, Projecting the impact of climate change on design recommendations for residential buildings in Iran, *Build. Environ.* 155 (2019) 283–297, doi:10.1016/j.buildenv.2019.03.053.
- [23] K.T. Huang, R.L. Hwang, Future trends of residential building cooling energy and passive adaptation measures to counteract climate change: the case of Taiwan, *Appl. Energy* 184 (2016) 1230–1240, doi:10.1016/j.apenergy.2015.11.008.
- [24] R.L. Hwang, W.M. Shih, T.P. Lin, K.T. Huang, Simplification and adjustment of the energy consumption indices of office building envelopes in response to climate change, *Appl. Energy* 230 (2018) 460–470, doi:10.1016/j.apenergy.2018.08.090.
- [25] X. Wang, D. Chen, Z. Ren, Assessment of climate change impact on residential building heating and cooling energy requirement in Australia, *Build. Environ.* 45 (2010) 1663–1682, doi:10.1016/j.buildenv.2010.01.022.
- [26] M. Kottke, J. Grieser, C. Beck, B. Rudolf, F. Rubel, World map of the Köppen-Geiger climate classification updated, *Meteorologische Zeitschrift* 15 (2006) 259–263, doi:10.1127/0941-2948/2006/0130.
- [27] Hong Kong Observatory, The Year's Weather - 2018, Hong Kong, 2019. <https://www.weather.gov.hk/wxinfo/pastwx/2018/ywx2018.htm> [accessed 15.04.2019].
- [28] Development Bureau, Transport and Housing Bureau, Energy Saving Plan For Hong Kong's Built Environment 2015–2025+, Environment Bureau, 2015.
- [29] S.L. Wong, K.K.W. Wan, D.H.W. Li, J. Lam, Impact of climate change on residential building envelope cooling loads in subtropical climates, *Energy Build* 42 (2010) 2098–2103, doi:10.1016/j.enbuild.2010.06.021.
- [30] K.S.Y. Wan, F.W.H. Yik, Building design and energy end-use characteristics of high-rise residential buildings in Hong Kong, *Appl. Energy* 78 (2004) 19–36, doi:10.1016/S0306-2619(03)00103-X.
- [31] Environment Bureau, Hong Kong's Climate Action Plan 2030+, Hong Kong, 2017. www.climate.gov.hk [accessed 18.01.2019].
- [32] BEAM, BEAM Plus New Buildings Version 1.2, HKGBC and BEAM Society Limited, 2012. <https://www.beamsociety.org.hk/files/download/download-20130724174420.pdf> [accessed 18.04.2019].
- [33] J.C. Lam, K.K.W. Wan, T.N.T. Lam, S.L. Wong, An analysis of future building energy use in subtropical Hong Kong, *Energy* 35 (2010) 1482–1490, doi:10.1016/j.energy.2009.12.005.
- [34] W.Y. Fung, K.S. Lam, W.T. Hung, S.W. Pang, Y.L. Lee, Impact of urban temperature on energy consumption of Hong Kong, *Energy* 31 (2006) 2623–2637, doi:10.1016/j.energy.2005.12.009.
- [35] B.W. Ang, H. Wang, X. Ma, Climatic influence on electricity consumption: the case of Singapore and Hong Kong, *Energy* 127 (2017) 534–543, doi:10.1016/j.energy.2017.04.005.
- [36] T.E. Morakinyo, C. Ren, Y. Shi, K.K.L. Lau, H.W. Tong, C.W. Choy, E. Ng, Estimates of the impact of extreme heat events on cooling energy demand in Hong Kong, *Renew. Energy* 142 (2019) 73–84, doi:10.1016/j.renene.2019.04.077.
- [37] A.L.S. Chan, Developing future hourly weather files for studying the impact of climate change on building energy performance in Hong Kong, *Energy Build.* 43 (2011) 2860–2868, doi:10.1016/j.enbuild.2011.07.003.
- [38] L. Troup, D. Fannon, Morphing climate data to simulate building energy consumption, in: Proceedings of the ASHRAE and IBSPA-USA SimBuild Building Performance Modeling Conference, Atlanta, USA, 2016.
- [39] A.L.S. Chan, T.T. Chow, S.K.F. Fong, J.Z. Lin, Generation of a typical meteorological year for Hong Kong, *Energy Conv. Manag.* 47 (2006) 87–96, doi:10.1016/j.enconman.2005.02.010.
- [40] T.C. Lee, K.Y. Chan, W.L. Ginn, Projection of extreme temperatures in Hong Kong in the 21st century, *Acta Meteorologica Sinica* 25 (2011) 1–20, doi:10.1007/s13351-011.
- [41] K.E. Taylor, R.J. Stouffer, G.A. Meehl, An overview of CMIP5 and the experiment design, *Bulletin of the American Meteorological Society* 93 (2012) 485–498, doi:10.1175/BAMS-D-11-00094.1.
- [42] H.S. Chan, H.W. Tong, Temperature projection for Hong Kong in the 21st century using CMIP5 models, in: Proceedings of the 28th Guangdong-Hong Kong-Macao Seminar on Meteorological Science and Technology, Hong Kong, 2014 13–15 January.
- [43] H.W. Tong, C.P. Wong, S.M. Lee, Projection of wet-bulb temperature for Hong Kong in the 21st century using CMIP5 data, The 31st Guangdong - Hong Kong - Macao Seminar on Meteorological Science and Technology and The 22nd Guangdong - Hong Kong - Macao Meeting on Cooperation in Meteorological Operations, 2017 27 February - 1 March.
- [44] Y. Xu, C.H. Xu, Preliminary assessment of simulations of climate changes over China by CMIP5 multi-models, *Atmos. Ocean. Sci. Lett.* 5(2012) 489–494, doi:10.1080/16742834.2012.11447041.
- [45] X.J. Gao, M.L. Wang, G. Filippo, Climate change over China in the 21st century as simulated by BCC_CSM1.1-RegCM4.0, *Atmos. Ocean. Sci. Lett.* 6(2013) 381–386, doi:10.3878/j.issn.1674-2834.13.0029.
- [46] R. Pincus, C.P. Batstone, R.J.P. Hofmann, K.E. Taylor, P.J. Glecker, Evaluating the present-day simulation of clouds, precipitation, and radiation in climate models, *J. Geophys. Res.* 113 (2008) D14209, doi:10.1029/2007JD009334.
- [47] D.W. Pierce, T.P. Barnett, B.D. Santer, P.J. Gleckler, Selecting global climate models for regional climate change studies, in: Proceedings of the National Academy of Sciences of the United States, 106, 2009, pp. 8441–8446, doi:10.1073/pnas.0900094106.
- [48] G.P. Peters, R.M. Andrew, T. Boden, J.G. Canadell, P. Ciais, C.L. Quéré, et al., The challenge to keep global warming below 2°C, *Nat. Clim. Chang.* 3 (2012) 4–6, doi:10.1038/nclimate1783.
- [49] M. Zhu, Y. Pan, Z. Huang, P.Xu Z., An alternative method to predict future weather data for building energy demand simulation under global climate change, *Energy Build.* 113 (2016) 74–86, doi:10.1016/j.enbuild.2015.12.020.
- [50] Hong Kong Housing Authority, Housing authority property location and profile, 2019. <https://www.housingauthority.gov.hk/en/global-elements/estate-locator/index.html> [accessed 24.03.2019].
- [51] Y. Tan, G. Liu, Y. Zhang, C. Shuai, G.Q. Shen, Green retrofit of aged residential buildings in Hong Kong: a preliminary study, *Build. Environ.* 143 (2018) 89–98, doi:10.1016/j.buildenv.2018.06.058.
- [52] Hong Kong Housing Authority, HKHA Annual Report 2017 / 2018.
- [53] Hong Kong Housing Authority, Housing Authority Public Housing Portfolio, 2018.
- [54] N.M. Mateus, A. Pinto, G.C.D. Graça, Validation of Energyplus thermal simulation of a double skin naturally and mechanically ventilated test cell, *Energy Build.* 75 (2014) 511–522, doi:10.1016/j.enbuild.2014.02.043.
- [55] S. Liu, Y.T. Kwok, K.K.L. Lau, P.W. Chan, E. Ng, Investigating the energy saving potential of applying shading panels on opaque façades: a case study for residential buildings in Hong Kong, *Energy Build.* 193 (2019) 78–91, doi:10.1016/j.enbuild.2019.03.044.
- [56] Y.T. Kwok, A.K.L. Lai, K.K.L. Lau, P.W. Chan, Y. Lavafpour, J.C.K. Ho, E. Ng, Thermal comfort and energy performance of public rental housing under typical and near-extreme weather conditions in Hong Kong, *Energy Build.* 156 (2017) 390–403, doi:10.1016/j.enbuild.2017.09.067.
- [57] H. Chen, W.L. Lee, F.W.H. Yik, Applying water cooled air conditioners in residential buildings in Hong Kong, *Energy Conv. Manag.* 49 (2008) 1416–1423, doi:10.1016/j.enconman.2007.12.024.
- [58] P. Xue, C.M. Mak, Y. Huang, Quantification of luminous comfort with dynamic daylight metrics in residential buildings, *Energy Build.* 117 (2016) 99–108, doi:10.1016/j.enbuild.2016.02.026.
- [59] X. Chen, Yang H, Zhang W, A comprehensive sensitivity study of major passive design parameters for the public rental housing development in Hong Kong, *Energy* 93 (2015) 1804–1818, doi:10.1016/j.energy.2015.10.061.
- [60] M.P. Deuble, R.J. de Dear, Mixed-mode buildings: a double standard in occupants' comfort expectations, *Build. Environ.* 54 (2012) 53–60, doi:10.1016/j.buildenv.2012.01.021.
- [61] M. Orme, M.W. Liddament, A. Wilson, Numerical Data for Air Infiltration & Natural Ventilation Calculations, International Energy Agency, Air Infiltration and Ventilation Centre, 1998.
- [62] D.W. Pieter, T. Wei, The role of adaptive thermal comfort in the prediction of the thermal performance of a modern mixed-mode office building in the UK under climate change, *J. Build. Perform. Simul.* 3 (2010) 87–101, doi:10.1080/19401490903486114.
- [63] K.J. Lomas, Y. Ji, Resilience of naturally ventilated buildings to climate change: advanced natural ventilation and hospital wards, *Energy Build.* 41(2009) 629–653, doi:10.1016/j.enbuild.2009.01.001.
- [64] S.G. Daniel, R.B. Carlos, J.M.R. Juan, P.F. Alexis, Towards the quantification of energy demand and consumption through the adaptive comfort approach in mixed mode office buildings considering climate change, *Energy Build.* 187 (2019) 173–185, doi:10.1016/j.enbuild.2019.02.002.
- [65] M. Luo, B. Cao, J. Damiens, B. Lin, Y. Zhu, Evaluating thermal comfort in mixed-mode buildings: a field study in a subtropical climate, *Build. Environ.* 88 (2015) 46–54, doi:10.1016/j.buildenv.2014.06.019.
- [66] ASHRAE, ASHRAE standard 55: thermal environmental conditions for human occupancy, American Society of Heating, Refrigerating and Air-Conditioning Engineers, 2017.
- [67] M. Herrera, S. Natarajan, D.A. Coley, T. Kershaw, A.P.R. Gonzalez, M. Eames, D. Fosas, M. Wood, A review of current and future weather data for building simulation, *Build. Serv. Eng. Res. Technol.* 38(2017) 602–627, doi:10.1177/0143624417705937.
- [68] M. Santamouris, A. Sfakianaki, K. Pavlou, On the efficiency of night ventilation techniques applied to residential buildings, *Energy Build.* 42 (2010) 1309–1313, doi:10.1016/j.enbuild.2010.02.024.

- [69] C. Buratti, R. Mariani, E. Moretti, Mean age of air in a naturally ventilated office: experimental data and simulations, *Energy Build.* 43 (2011) 2021–2027, doi:[10.1016/j.enbuild.2011.04.015](https://doi.org/10.1016/j.enbuild.2011.04.015).
- [70] C.C. Federspiel, Air-change effectiveness, theory and calculation methods, *Indoor Air* 9 (1999) 47–56, doi:[10.1111/j.1600-0668.1999.t01-3-00008.x](https://doi.org/10.1111/j.1600-0668.1999.t01-3-00008.x).
- [71] A. Novoselac, J. Srebric, A critical review on the performance and design of combined cooled ceiling and displacement ventilation systems, *Energy Build.* 34 (2002) 497–509, doi:[10.1016/S0378-7788\(01\)00134-7](https://doi.org/10.1016/S0378-7788(01)00134-7).